

MCU-based Battery Health Diagnostic System using Electrochemical Impedance Spectroscopy and Regression Models

Goodwill Gwala (674390)
Vuyiswa Gwadiso (1259616)
Goitseona Mohajane(1027296)
Project Group 13, 12 July 2020

The University of the Witwatersrand, Johannesburg, South Africa
School of Electrical and Information Engineering

Abstract— A microcontroller-based Battery Diagnostic System that estimates the health of a battery using EIS techniques and regression models is presented. A signal generator and signal conditioning circuitry are implemented, including a Data Acquisition System to monitor the EIS response. FFT and Logarithmic Regression transformations algorithms are developed through embedded software. A system accuracy of 87.6% and a run-time of less than 30ms is achieved through experimental testing. This system is best suited for quality control in industrial applications. Measurement accuracy could be improved by using a controlled temperature chamber, introducing a calibration system and attaching external memory which are recommendations for further development.

I. INTRODUCTION

Fast and reliable battery health estimation techniques are increasingly becoming an important field of interest due to the rapid growth of renewable energy. AA Batteries are essential components of most electronic devices [1].

A Battery Diagnostic System (BDS) that accurately estimates the health of these components is vital in ensuring safe and reliable performance. A BDS that estimates the health of AA batteries using EIS by modelling the relationship between Internal Resistance and the State-of-Charge (SOC) using non-linear regression is presented.

A brief overview of the EIS technique is discussed. Technical specifications, design considerations and constraints, system requirements and success criteria are established. A design overview and methodology is presented. A thorough design consideration and implementation of circuit models, Data Acquisition (DAQ) system, modelling tools and algorithms used to predict the State-of-Health (SOH) of any given AA battery is discussed. The design is implemented and validated through modular design and testing, and evaluated through critical analysis. The results are presented and future recommendations are made. Project scheduling and planning is presented in Figure 3 in Appendix A

II. BACKGROUND

EIS is a widely used standard characterisation technique for a variety of applications [2]. EIS is an AC perturbative characterisation technique used to establish the dynamic electrical response of chemical systems such as batteries [3].

Quantitative measurements produced by the EIS can be used in the evaluation of small scale chemical mechanisms such as impedance. This is a tried and tested method verified by the likes of E. Barsoukov *et al* [3] and A. Densmore *et al* [4], which proves to yield quick yet accurate results. The design of the BDS is expected to adhere to the requirements, technical specifications and constraints prescribed by the project brief [5]. The speed, reliability and accuracy of the system will dictate its success. The proposed system has both commercial and industrial potential applications, however it is best suited for quality control in industrial applications.

III. METHODOLOGY & DESIGN OVERVIEW

The basic operating principle of the diagnostic system is to provide an excitation signal, monitor the EIS response of the battery through signal conditioning circuitry and a DAQ system. The general approach for predicting the SOH is to acquire a model of a test battery using the DAQ processes, the model is acquired by monitoring the EIS response periodically in fixed time intervals corresponding to different SOC. The model can also be developed from information obtained from the manufacturers. The model is added to a database of models. The SOH of a similar battery can be predicted by simply monitoring their impedance. Figure 1 below illustrates the overview of the design and describes the processes and constituent elements involved in the estimation of the SOH.

The signal conditioning circuitry comprises of a current

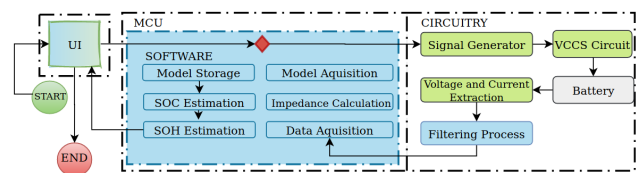


Fig. 1. Design Overview

sink and filters. The MCU facilitates data acquisition through an appropriately configured ADC. The embedded software provides the implementation of algorithms that predict the

SOH of the battery under test. The results are displayed through the User Interface (UI).

IV. USER INTERFACE

A. Project Target Market

The proposed system application in the commercial industry allows the end-user to easily retrieve the battery State Of Health (SOH). This is achieved by allowing the end-user to get result analysis in terms of the SOH displayed as a percentage. The SOH percentage is further categorised into three states, excellent, good and bad allowing a commercial user to easily interpret the results. The proposed system in industrial application allows the end-user to acquire other battery system models. There are different types of AA batteries [6]. The models are acquired by means of EIS and regression models and the model is thus saved.

B. User Interface LCD Screen

The user interacts with the software by means of LCD screen. The LCD screen used for this project is the, LCD shield for Arduino (SHD036) [7]. The screen is shown in figure 13, appendix E. This LCD screen is chosen due to its compatibility with the Atmega328p and the number of buttons it offers which allows the end-user to easily interact with the software.

C. LCD Screen Menu

The battery test is subdivided into quick test and long test. Results menu is subdivided into battery voltage and impedance. The program menu is subdivided into lithium and NiMH to allow the user to acquire a model. The program option can be further advanced by creating more options, hence the code is written in such a way that separation of layers and concern is prioritised. The front-end calls the the necessary data layer functions and displays the results.

V. CIRCUIT MODELS

The signal generator produces a excitation signal and two design considerations where made, the RC phase shift oscillator and the Wein Bridge oscillator [8]. Based on the design requirements the RC phase shift oscillator was chosen because it is cost effective,low power consumption, and good frequency and amplitude stability [9]. The block diagram of the RC phase shift oscillator is illustrated in Appendix C figure 8. A 3 stage RC phase-shifting network is used to determine the required frequency of the sine wave hence the values of R and C have been chosen so to generate a frequency of 1000 Hz, the frequency is determined using Eq.1.

$$F = \frac{1}{2\pi RC\sqrt{2N}} \quad (1)$$

To maintain a continuous constant frequency sine wave at the output the design has a total phase shift of 2π radians from the common emitter amplifier and the 3 stage feedback network thus satisfying Barhausen's criterion [10]. A DC offset circuitry is designed to produce an offset of 100mV as illustrated in the block diagram in Appendix

C figure 9. The complete circuitry of the signal generator design is illustrated in Appendix C figure 10. The signal generator starts with an initial voltage noise, which affects the stability of frequency and sine wave amplitude thus outputting unwanted DC offsets. To avoid loading effect when the signal generator is connected to the VCCS, the output impedance of the function generator is assumed to be very small compared to that of the VCCS. The design does meet the required specifications to produce a sine wave with amplitude of 200mV and a DC offset of 100mV as illustrated in Appendix C figure 11.

A low power-consumption voltage-controlled current sink (VCCS) with high precision, low noise distortion and provides stability over a range of temperatures and load variations is required. Several VCCS circuit were considered, including amplifier BJT combinations as well as the darlington pair configuration. Based on the design requirements a MOSFET and Op amp configuration is implemented.

The ADA4805 is employed as it provides high precision, low harmonic distortion which improves accuracy, low offset voltage and low bias currents [11]. The IRF620 is employed as it facilitates a low power consumption design [12]. A high precision power resistor is used as well as provides stability against temperature changes and improves overall measurement accuracy. The current sink model is shown in Appendix A, Figure 4.

VI. DATA ACQUISITION

A low-cost, power conservative, multi-channel data acquisition system with an integrated ADC, GUI support, embedded memory for data manipulation and storage is required. The commercially available ATmega328P microprocessor is considered as it meets these specifications [13]. The DAQ system constituent elements and processes is illustrated by Figure 1 in Appendix A. The ADC facilitates the sampling of data for each channel and is configured for the desired adequate sampling rates and resolution of 125kHz and 10-bits respectively.

The real-time signal processing of the DAQ system is realised through embedded software programming. Discrete Fourier Transform techniques, using a FFT algorithm and Windowing on the measured and conditioned signals, are applied [15]. The amplitudes of the signals are easily extracted from the frequency information obtained from the FFT process and are used in the AC impedance calculation and model acquisition process.

A modelling tool that adequately encapsulates the dynamic characteristics of a battery is required. The Model Acquisition process is realised through Logarithmic Regression (LR), a statistical learning algorithm. Regression modelling is a predictive analysis method that models the relationship between a dependent (Impedance) and

Independent (SOC) variable [14] [19]. Initially a linear regression model was considered, however this model failed to capture the non-linear characteristics. An improved LR technique is employed illustrated by Eq.2 [19].

$$Y_i = \alpha + \beta \log X_i + \epsilon_i \quad (2)$$

where Y_i represents a specific SOC estimate for a specific measure of impedance X_i . The regression coefficients, α and β , represents the unbiased estimates for the intercept (model boundary) and gradient respectively. The model interpretation of the estimated coefficient β is that a unit change in the impedance will produce an expected change in β units. This model is stored in the EEPROM. The SOH can be determined by using Eq.3.

$$SOH = e^{\left(\frac{Y_i - \beta}{\alpha} \times \epsilon_i\right)} \times 100\% \quad (3)$$

where SOH represents the predicted health percentage for a specific estimate of SOC based on the measured impedance in real-time. The regression error coefficient ϵ_i represents the unbiased voltage error estimate.

VII. RESULTS AND ANALYSIS

The experimental set up is presented by Figure 12 in Appendix B. The discharge characteristics are observed in Figure 5 in Appendix B. The simulated model proves to be a good approximation of the behaviour of an actual battery. The minor discrepancies observed are attributed to the tolerance errors, crosstalk interference in the DAQ system, temperature drifts, errors due to contact measuring, and non-ideal components and environment [2].

ADC measurements contain a variety of unavoidable, independent errors that have an impact on the accuracy that can be achieved. A sample ADC experimental result is presented by Figure 6 in Appendix D and also illustrates quantization error. Due to the low frequency nature of the excitation signal the response signal is adequately sampled at $10\times$ the Nyquist frequency, the collective encountered errors are relatively small. The observed discrepancies are attributed to gain, linearity, missing code and offset errors encountered during the experiment. Most of these errors are inherent to ADC's, however measurement accuracy could be improved by introducing a calibration system to adjust the gain and offset. A method called dithering could potentially be implemented in the future [15].

The sampled data undergoes a frequency transformation by performing a FFT function with Windowing and digital filtering to retrieve the magnitude information of the response signal. The measured and simulated results are illustrated by Figure 7, Appendix B. There is evidence of amplitude error attributed to Coherent Power Gain errors due to windowing, Scalloping Losses due to frequency discretization errors and system noise. There is also evidence of spectral leakage attributed to the number of samples the MCU is able to handle due to memory limitations. These errors can be

addressed by implementing a windowing function with a better Equivalent Noise Bandwidth correction factor and attaching an external memory which is a recommendation for further development [15] [16] [17].

The model acquisition results shown in Figure 2 illustrates the non-linear characteristics of a battery. Both models are relatively linear and exhibit increasing non-linearity with a decrease in SOC. The experimental model closely captures these characteristics. The experimental model becomes highly non-linear as SOC is depleted, hence this qualifies Logarithmic Regression modelling. These errors are attributed to non-ideal components and environment as well as increase in temperature. A controlled temperature chamber could be used during model acquisition to minimise these errors. The accuracy analysis, repeatability and reproducibility of the system are illustrated by Table I below.

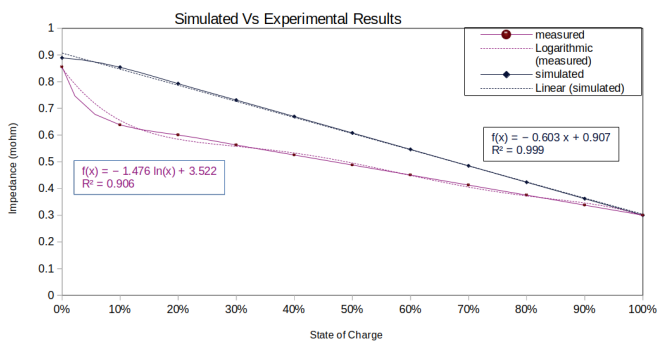


Fig. 2. AC Impedance Vs SOC

TABLE I
ACCURACY ANALYSIS OF BATTERY DIAGNOSTIC SYSTEM

Control	Samples	Avg	Ω Error(%)	SOH Error(%)
0.41 Ω	1	0.38 Ω	6.8	12.4
0.41 Ω	5	0.39 Ω	3.2	12.2
0.41 Ω	10	0.42 Ω	2.7	11.0

The errors decrease as the number of samples increase demonstrating consistent repeatability and reproducibility. The predicted SOH of the battery determined using the model acquired demonstrates some error correcting due to the error coefficient as illustrated by Eq.3. The proposed BDS can predict the health of any given AA battery with approximately 87.6% accuracy in less than 30ms, based on a timed experiment. The design is considered a success but better accuracy could be achieved, recommendations for further development are outlined.

VIII. CONCLUSION

A design of a microcontroller-based battery health diagnostic system using Electrochemical Impedance Spectroscopy and Regression Models is presented. The experimental results show that the proposed Battery Diagnostic System can predict the health of any given AA battery with approximately 87.6% accuracy in less than 30ms.

REFERENCES

- [1] P. Lu, M. Li, L. Zhang and L. Zhou, "A Novel Fast-EIS Measuring Method And Implementation for Lithium-ion Batteries," 2019 Prognostics and System Health Management Conference (PHM-Qingdao), Qingdao, China, 2019, pp. 1-600.
- [2] Battery Technology Handbook, Second Edition, H. A. Kiehne, 2003.
- [3] E. Barsoukov and J. R. Macdonald, "Impedance Spectroscopy Theory Experiment and Applications" in , Wiley, 2005.
- [4] A. Densmore and M. Hanif, "Determining battery SOC using Electrochemical Impedance Spectroscopy and the Extreme Learning Machine," 2015 IEEE 2nd International Future Energy Electronics Conference (IFEEC), Taipei, 2015, pp. 1-297.
- [5] K Nixon School of Electrical and Information Engineering. (01/7/2020) elen3017-proj-addendum-2020.pdf
- [6] Kimberly Hawthorne, "Why not mix two types of double battery?", "<https://sciencing.com/not-two-types-aa-batteries-8523093.html>".
- [7] "<http://www.mantech.co.za/datasheets/products/SHD036.pdf>"
- [8] Bhargava N N, Kulshrestha D C, Gupta S C, "Basic Electronics and Linear Circuits", second edition,pp 415-420.
- [9] D Wen, "Analysis of the RC Phase-shift Oscillator", 2019 12th International Congress on Image and Signal Processing, Biomedical Engineering and Informatics (CISP-BMEI), Suzhou, China, 2019, pp.1-4,doi: 10.1109/CISP-BMEI48845.2019.8966078.
- [10] Salivahanan S, Suresh Kumar N, Vallavaraj A, "Electronic Devices and Circuits", 1998, pp 424.
- [11] Analog Devices "High speed voltage feedback rail-to-rail output amplifier" ADA4805 datasheet, Nov. 1999 [Revised Sept 2009]
- [12] Vishay Siliconix "Power MOSFET" IRF620 datasheet, Nov. 1997 [Revised Mar 2011]
- [13] Atmel "8-bit AVR Microcontroller" ATmega328P datasheet, Nov. 2016 [Revised Mar 2020]
- [14] Kavitha S, Varuna S and Ramya R, "A comparative analysis on linear regression and support vector regression," 2016 Online International Conference on Green Engineering and Technologies (IC-GET), Coimbatore, 2016, pp. 1-5.
- [15] Data acquisition handbook. Measurement Computing Corporation. 2012.
- [16] R. Lyons, Reducing FFT Scalloping Loss Errors Without Multiplication [DSP Tips and Tricks],Signal Processing Magazine, IEEE , vol. 28, pp. 50-116, March 2011.
- [17] Charles L. Phillips and H. Troy Nagle. 1995. Digital control system analysis and design (3rd ed.). Prentice-Hall, Inc., USA.
- [18] F. Harris, On the use of windows for harmonic analysis with the discrete Fourier transform,in Proceedings of the IEEE , vol. 66, 1978/2005.
- [19] Prykhodko, N. Prykhodko and L. Makarova, "Building the Non-Linear Regression Equations on the basis of Multivariate Normalizing Transformations", Proceedings of the 2018 IEEE First International Conference on System Analysis & Intelligent Computing (SAIC-2018), October 08–12, 2018.

I. APPENDIX A

The design process of a microcontroller-based Battery Diagnostic System that estimates the health of a battery using EIS techniques and regression models is documented below. Project planning and scheduling and a detailed design overview is presented. Design considerations of the Current Sink Circuit model and results are presented below.

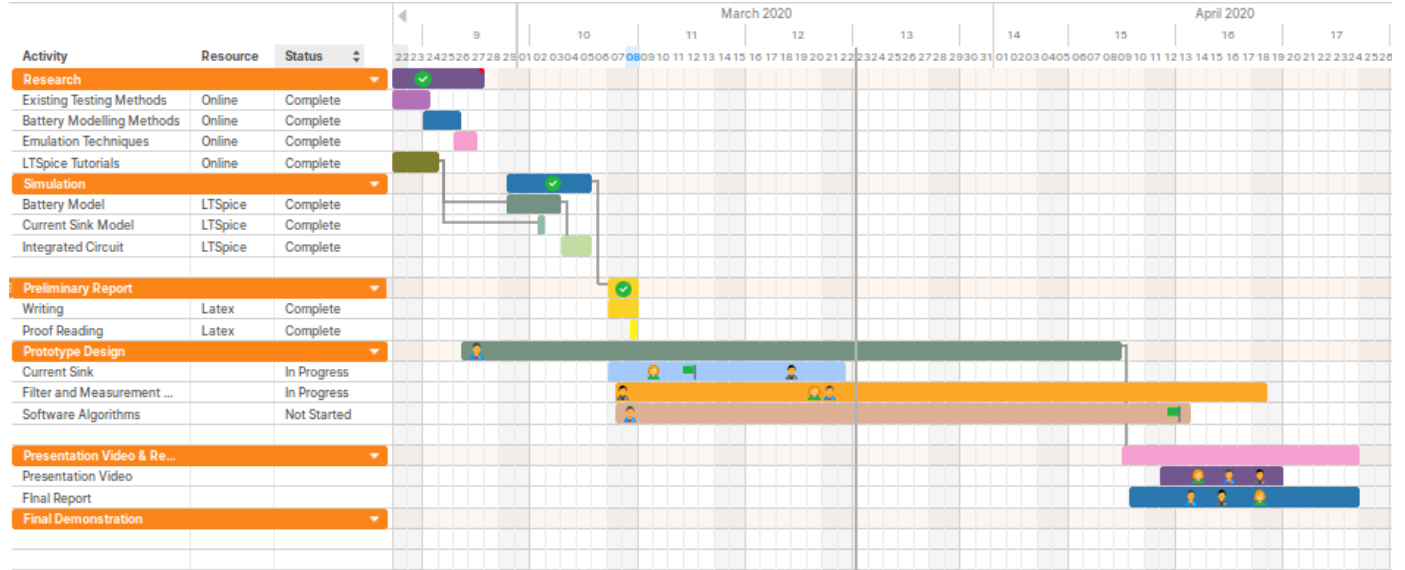


Fig. 3. Project Planning & Work Division

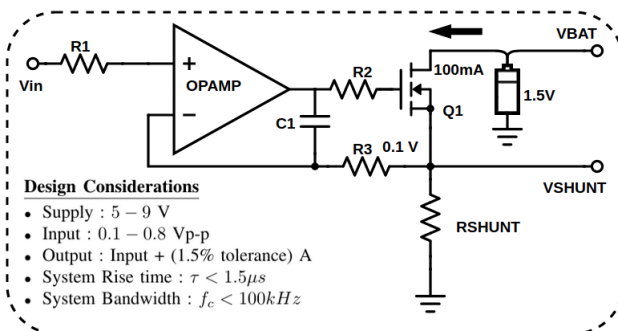


Fig. 4. Current Sink Circuit Model

TABLE II
CIRCUIT MODELS MEASUREMENTS

Parameter	Simulated	Measured	Error(%)
Input	0.2 Vp-p	0.21 Vp-p	0.05
Output	100 mA	102 mA	0.02
System Bandwidth	10MHz	8MHz	20
System rise-time	1.5 μs	2.7 μs	50

II. APPENDIX B

This Appendix documents the results of a Battery Diagnostic System through the DAQ system. The measured and simulated results of the battery discharge model, ADC sampling as well as the FFT results are presented below.

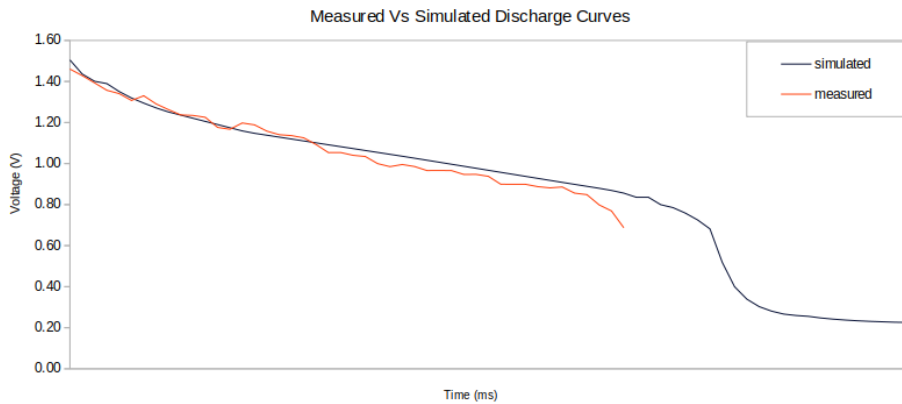


Fig. 5. Discharge Curves of Simulated and Experimental Battery Model

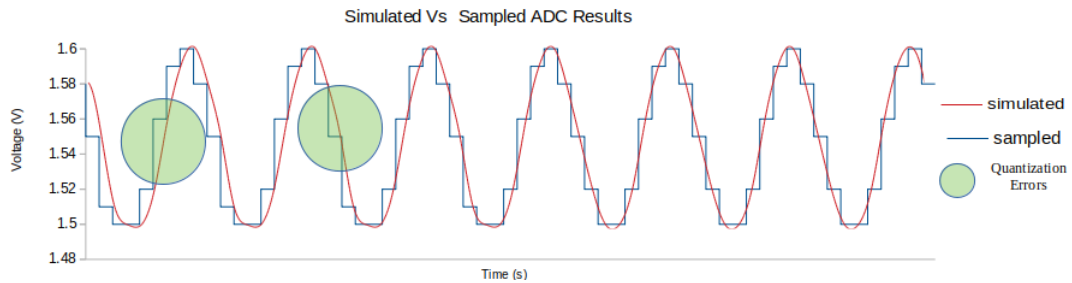


Fig. 6. ADC Results showing magnitudes and errors

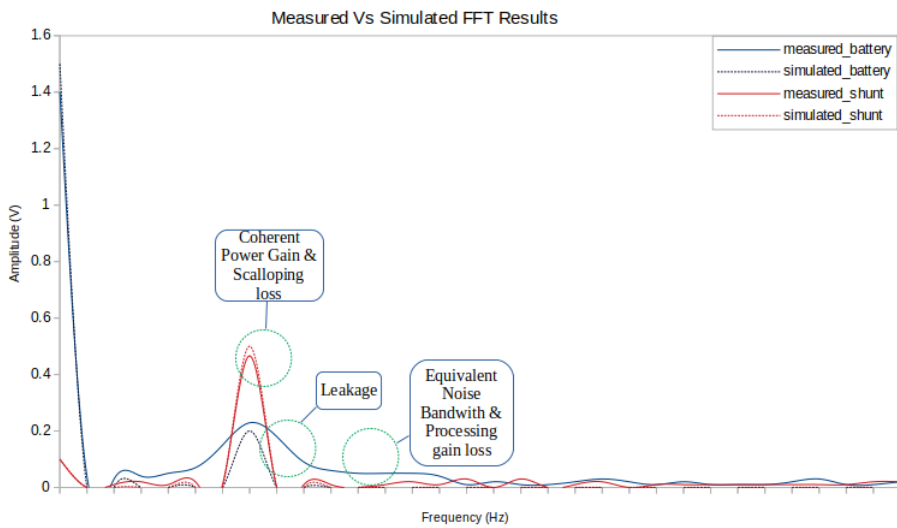


Fig. 7. FFT Results showing magnitudes and errors

III. APPENDIX C

Appendix C presents the sine wave generator design, blocks diagrams of the design, circuitry and simulation results.

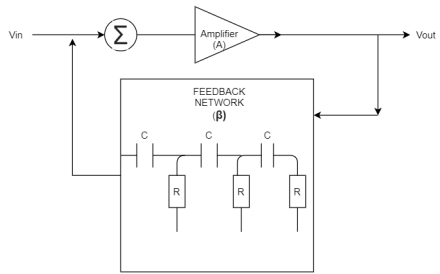


Fig. 8. Block diagram of the RC phase shift oscillator

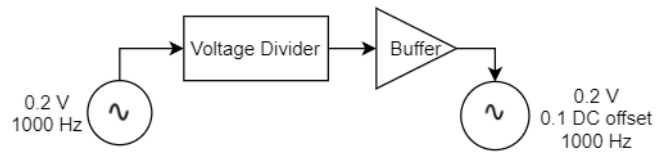


Fig. 9. Block diagram of DC offset

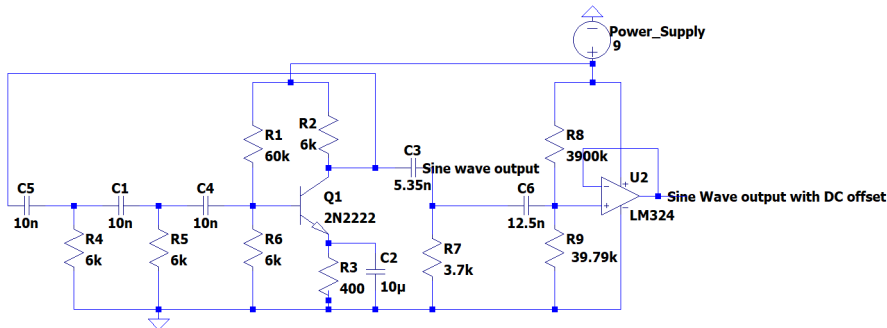


Fig. 10. The sine wave generator circuit

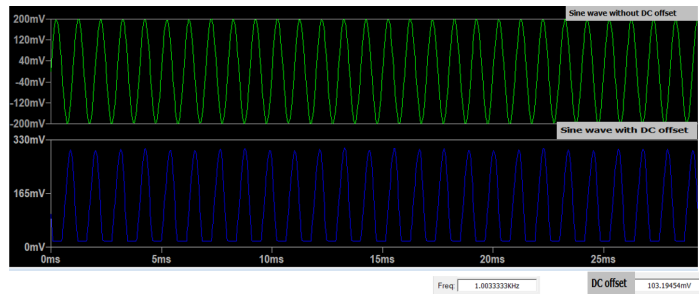


Fig. 11. Sine wave generator simulation Results

IV. APPENDIX D

Appendix D documents the experimental set up for the Battery Diagnostic System. An illustration of the Data Acquisition System and Current sink is presented. The Graphic User Interface is also demonstrated below.

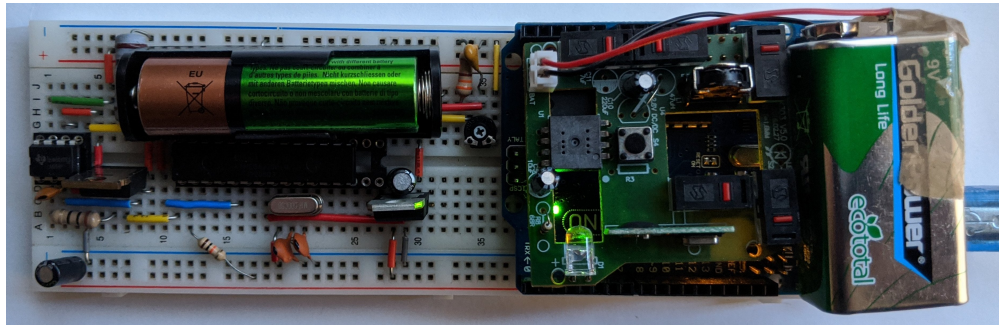


Fig. 12. DAQ Experimental Set Up

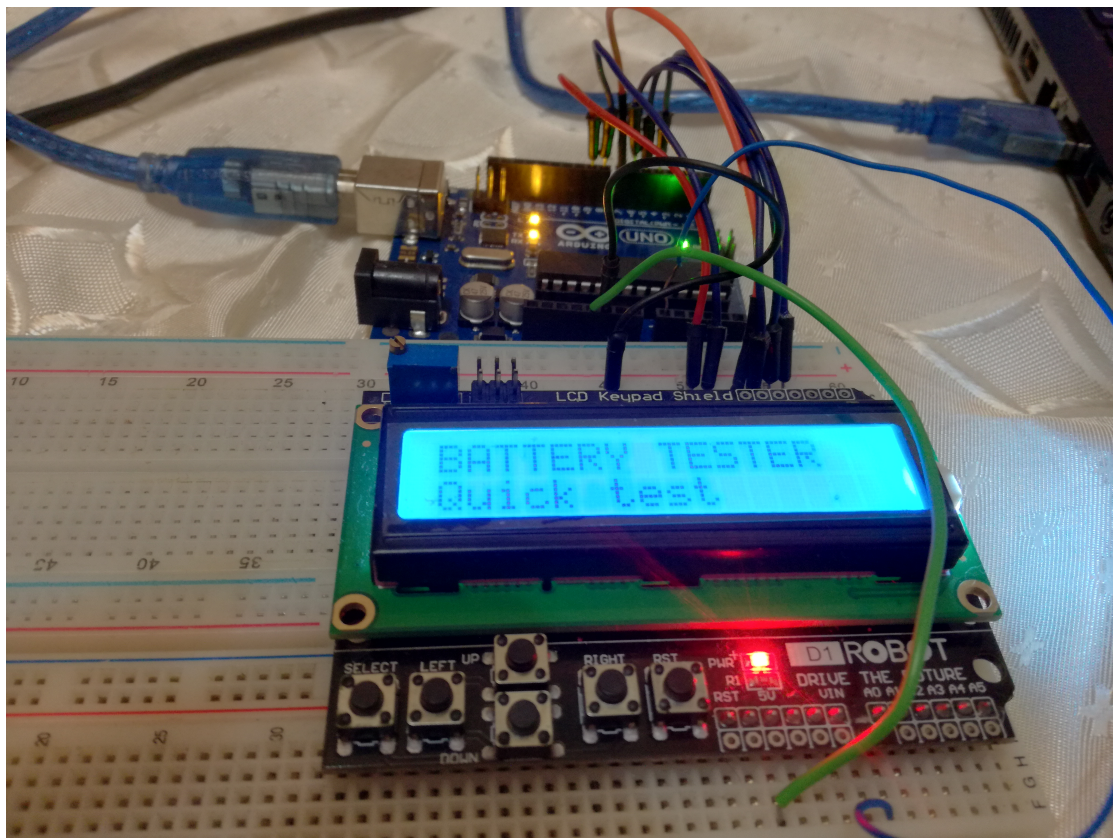


Fig. 13. LCD Screen Setup